УДК 621.382:539.3

OPTIMIZATION OF LASER SPLITTING PARAMETERS OF SILICATE GLASSES WITH ELLIPTICAL BEAMS IN THE PLANE OF PARALLEL SURFACE

Y. V. NIKITYUK, A. N. SERDYUKOV
Francisk Skorina Gomel State University,
the Republic of Belarus

I. Y. AUSHEV
State Educational Institution "University of Civil Protection of the Ministry for Emergency Situations of the Republic of Belarus", Minsk

Regression and neural network models of the process of laser splitting of silicate glasses by elliptical beams in a plane parallel to the surface were obtained. To conduct a numerical experiment, a central compositional plan was used. The processing speed, laser beam power and its geometric parameters were selected as variable factors. As responses, the values of maximum temperatures and the values of maximum thermoelastic tensile stresses in the processing zone were determined, the calculation of which was performed using the APDL programming language. An effective architecture for an artificial neural network created using the TensorFlow program has been established. A comparative analysis of neural network and regression models was carried out. The influence of input parameters on responses was assessed. Using the MOGA algorithm of the ANSYS program, the optimal modes for the formation of laser-induced cracks by elliptical beams were determined, ensuring the effective implementation of parallel laser splitting of silicate glass.

Keywords: laser chopping, artificial neural network, optimization, MOGA, ANSYS.

ОПТИМИЗАЦИЯ ПАРАМЕТРОВ ЛАЗЕРНОГО РАСКАЛЫВАНИЯ СИЛИКАТНЫХ СТЕКОЛ ЭЛЛИПТИЧЕСКИМИ ПУЧКАМИ В ПЛОСКОСТИ, ПАРАЛЛЕЛЬНОЙ ПОВЕРХНОСТИ

Ю. В. НИКИТЮК, А. Н. СЕРДЮКОВ
Учреждение образования «Гомельский государственный университет имени Франциска Скорины»,
Республика Беларусь

И. Ю. АУШЕВ
Государственное учреждение образования «Университет гражданской защиты Министерства по чрезвычайным ситуациям Республики Беларусь», г. Минск

Получены регрессионные и нейросетевые модели процесса лазерного раскалывания силикатных стекол эллиптическими пучками в плоскости, параллельной поверхности. Для проведения численного эксперимента был использован центральный композиционный план. В качестве варьируемых факторов выбраны скорость обработки, мощность лазерного пучка и его геометрические параметры. В качестве откликов определялись значения максимальных температур и значения максимальных термоупругих напряжений растяжения в зоне обработки, расчет которых был выполнен с применением языка программирования APDL. Установлена эффективная архитектура искусственной *нейронной сети, созданной с использованием программы TensorFlow. Проведен сравнительный анализ нейросетевых и регрессионных моделей. Выполнена оценка влияния входных параметров на отклики. С использованием алгоритма MOGA программы ANSYS определены оптимальные режимы формирования эллиптическими пучками лазерно-индуцированных трещин, обеспечивающие эффективную реализацию параллельного лазерного раскалывания силикатного стекла.*

Ключевые слова: лазерное раскалывание, искусственная нейронная сеть, оптимизация, MOGA, ANSYS.

Introduction

Glass, with its unique combination of properties, is extensively employed in various industrial applications. Cutting is a fundamental procedure in glass manufacturing, serving to achieve the desired shape and dimensions of the final products. Of particular importance is the efficient production of thin glass plates. The conventional methods for manufacturing thin glass plates rely on mechanical cutting, a process that is associated with substantial material losses, limited efficiency, and diminished strength of the final glass products [1, 2].

Presently, laser cleaving techniques have gained significant prevalence in the industrial sector [1–10]. Brittle nonmetallic materials, such as silicate glasses, can be effectively processed with these tools. The parallel laser cleaving technique can be used in this instance to produce thin glass plates. The fundamental principle underlying this technique is the generation of a laser-induced crack parallel to the surface of the material being processed. This crack is formed as a consequence of the glass plate being heated with an elliptical laser beam. Previous research has been conducted on the parallel laser cleaving technique for cutting brittle nonmetallic materials, as documented in [1, 11–13].

The use of metamodels has proven to be effective in several scenarios for the purpose of optimizing laser processing parameters. Metamodels have the potential to ascertain the output parameters of laser processing without performing exhaustive calculations, through the application of regression or neural network models [14–16]. Furthermore, within the context of metamodeling, it is possible to determine the optimal laser processing parameters, which may involve the use of genetic algorithms [17–22].

There is a perceived necessity to conduct a more comprehensive examination of the parallel laser cleaving technique employed on silicate glasses. This investigation would involve the use of regression and neural network models to determine the optimal modes for generating laser-induced cracks that are parallel to the treated surface.

Determination of optimal parameters for glass cutting

APDL was used to compute the temperatures and thermoelastic stresses that arise in silicate glasses when subjected to an elliptical laser beam. This analysis was conducted within the context of the unbound thermoelasticity problem in the quasi-static problem statement [23, 24].

Figure 1 displays the schematic of spatial arrangement of the laser radiation impact zone. In Fig. 1, position *1* represents the laser beam with a wavelength of 10.6 microns, position *2* denotes the processed glass product, and position *3* represents the cross-section of the laser beam *1* in the cutting plane. The horizontal arrow indicates the direction of movement of the glass plate relative to the laser beam.

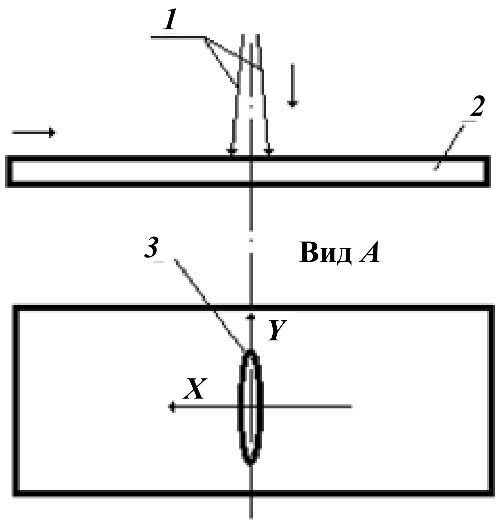

Fig. 1. Schematic of spatial arrangement
of the laser radiation impact zone

The following properties of silicate glasses were used for calculations: thermal conductivity $\lambda = 0.88$ W/m · K, specific heat capacity $C = 860$ J/kg · K, density $\rho = 450$ kg/m^3, thermal expansion coefficient $\alpha_T = 89 \cdot 10^{-7}$ (1/K), Young's modulus $E = 70$ GPa, Poisson's ratio $\nu = 0.22$ [25]. Finite element calculations were performed for a plate with dimensions of 0.025 × 0.02 × 0.002 m. The corresponding finite element model consisted of 69000 Solid 70 and Solid 185 elements utilized for thermal and strength analysis, respectively. The calculations were performed using the following parameters: V was set to 0.03 m/s, the laser power P was set to 10 W, the minor semi-axis of the laser beam A was set to $1 \cdot 10^{-3}$ m, and the major semi-axis B was set to $4 \cdot 10^{-3}$ m. Fig. 2, 3 illustrate the computed distributions of temperature fields and thermoelastic stress fields for the specified parameters of laser-induced heating of the silicate glass surface.

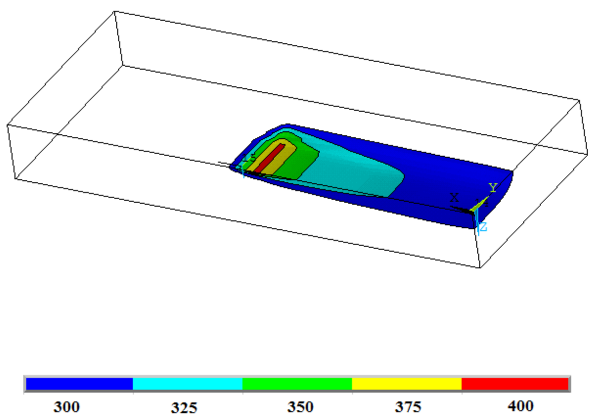

Fig. 2. Computed distribution of the temperature field under
the influence of an elliptical laser beam, K

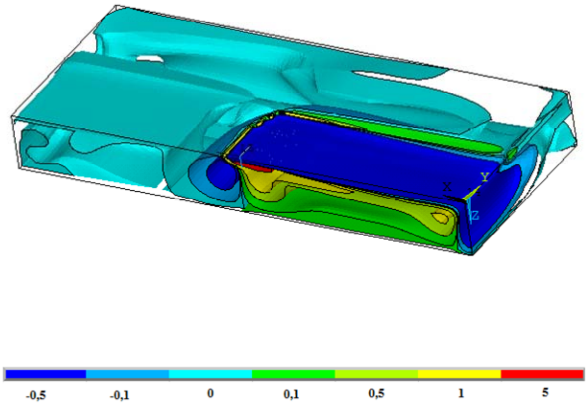

Fig. 3. Computed distribution of stresses σ_{zz} under the influence of an elliptical laser beam, MPa

The maximum calculated temperature does not exceed the glass transition temperature, which is equal to 789 K for silicate glass. This is a necessary condition for cutting glass via laser cleaving [25]. The presented distribution of stress fields σ_{zz} acting perpendicular to the treated surface reveals that a zone of compression stresses is formed in front of the elliptical beam center, and a zone of tensile stresses is formed in the depth of the glass, thus ensuring the generation of a laser-induced crack parallel to the surface of the glass plate. Here, the through-cut cleaving due to localization of stresses σ_{yy} in the sample (see Fig. 4) emerges as a noteworthy contender in comparison to laser glass delamination. The consideration of this particular circumstance is imperative in the determination of effective modes for parallel laser cleaving.

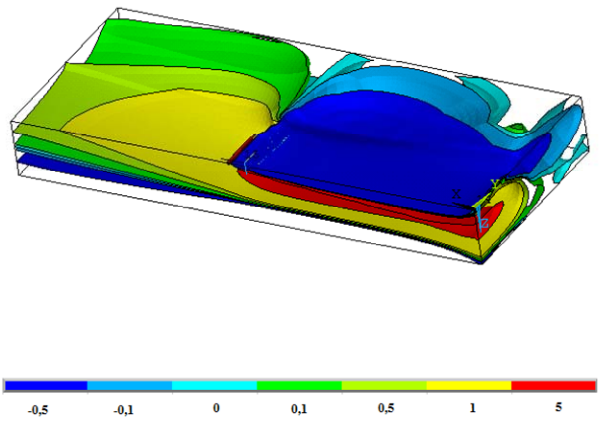

Fig. 4. Computed distribution of stresses σ_{yy} under the influence of an elliptical laser beam, MPa

The numerical experiment was carried out using 25 combinations of the face-centered version of the central composite design for four factors (*P*1–*P*4): *P*1 was the processing speed *V*, *P*2 was the laser power *P*, *P*3 was the minor semi-axis of the laser beam *A*, and *P*4 was the major semi-axis of the beam *B* (see Table 1). The following responses were determined: maximum temperature *T* and maximum tensile stresses σ_{yy} and σ_{zz} in the treatment zone.

Table 1

Experimental design and calculation results

No.	*P*1 *V*, m/s	*P*2 *P*, W	*P*3 *A*, m	*P*4 *B*, m	*P*5 *T*, K	*P*6 σ_{yy}, MPa	*P*6 σ_{zz}, MPa
1	0.015	15	0.0015	0.003	610	26.2	27.3
2	0.01	15	0.0015	0.003	687	31.7	26.7
3	0.02	15	0.0015	0.003	563	22.1	27.8
4	0.015	10	0.0015	0.003	504	17.4	18.2
5	0.015	20	0.0015	0.003	715	34.9	36.4
6	0.015	15	0.001	0.003	636	25.2	41.5
7	0.015	15	0.002	0.003	582	25.2	20.4
8	0.015	15	0.0015	0.002	768	38.8	41.5
9	0.015	15	0.0015	0.004	531	18.9	20.4
10	0.01	10	0.001	0.002	727	31.6	41.8
11	0.02	10	0.001	0.002	581	22.8	40.1
12	0.01	20	0.001	0.002	1160	63.3	83.7
13	0.02	20	0.001	0.002	868	45.6	80.3
14	0.01	10	0.002	0.002	647	29.0	20.2
15	0.02	10	0.002	0.002	540	21.6	20.8
16	0.01	20	0.002	0.002	1001	58	40.3
17	0.02	20	0.002	0.002	787	43.1	41.5
18	0.01	10	0.001	0.004	510	15.4	20.6
19	0.02	10	0.001	0.004	437	10.0	19.9
20	0.01	20	0.001	0.004	727	30.7	41.2
21	0.02	20	0.001	0.004	581	20.1	39.8
22	0.01	10	0.002	0.004	471	14.9	9.9
23	0.02	10	0.002	0.004	417	10.6	10.2
24	0.01	20	0.002	0.004	650	29.9	19.9
25	0.02	20	0.002	0.004	540	21.1	20.5

The corresponding regression equations that determine the relationship between the response functions (T, σ_{yy}, σ_{zz}) and the factors (V, P, A, B) are as follows:

$$Y_T = 7.10 - 4.75\cdot 10\cdot V + 8.73\cdot 10^{-2}\cdot P - 1.58\cdot 10^{-2}\cdot A - 4.30\cdot 10^{2}\cdot B +$$

$$+7.12\cdot 10^{2}\cdot V\cdot V - 6.62\cdot 10^{-4}\cdot P\cdot P + 4.43\cdot 10^{4}\cdot B\cdot B - 6.41\cdot 10^{-1}\cdot V\cdot P +$$

$$+4.12\cdot 10^{3}\cdot V\cdot A + 3.13\cdot 10^{3}\cdot V\cdot B - 2.89\cdot P\cdot A - 5.80\cdot P\cdot B + 1.56\cdot 10^{4}\cdot A\cdot B;$$

$$T = e^{YT} - 1;$$

$$Y_{sy} = 6.21\cdot 10^{2} - 8.83\cdot 10^{-3}\cdot V + 2.25\cdot 10\cdot P - 1.04\cdot 10^{5}\cdot B +$$

$$+1.24\cdot 10^{5}\cdot V\cdot V - 2.25\cdot 10^{-1}\cdot P\cdot P - 1.33\cdot 10^{7}\cdot A\cdot A + 9.10\cdot 10^{6}\cdot B\cdot B -$$

$$-1.09\cdot 10^{2}\cdot V\cdot P + 9.09\cdot 10^{5}\cdot V\cdot A - 1.15\cdot 10^{3}\cdot P\cdot B + 7.12\cdot 10^{6}\cdot A\cdot B;$$

$$\sigma_{yy} = \left(Y_{sy} \cdot 0.295 + 1\right)^{\left(\frac{1}{0.295}\right)} - 1;$$

$$Y_{sz} = 1.95 \cdot 10 + 1.60 \cdot 10^{-1} \cdot P - 1.51 \cdot 10^{3} \cdot A - 7.63 \cdot 10^{2} \cdot B -$$

$$- 2.83 \cdot 10^{-3} \cdot P \cdot P + 2.47 \cdot 10^{5} \cdot A \cdot A + 6.30 \cdot 10^{4} \cdot B \cdot B +$$

$$+ 7.32 \cdot 10^{2} \cdot V \cdot A;$$

$$\sigma_{zz} = \left(Y_{sz} \cdot 0.005 + 1\right)^{\left(\frac{1}{0.005}\right)} - 1.$$

The impact of factors on the response functions was evaluated (Fig. 5). All output parameters are considerably affected by the laser radiation power P and the length B of the major semi-axis of the elliptical beam during the implementation of parallel laser cleaving. Simultaneously, the maximum temperatures in the treatment zone T and the maximum tensile stresses σ_{yy} are significantly influenced by the processing speed V. Additionally, the maximum tensile stresses σ_{zz} are affected by the size A of the minor semi-axis of the laser elliptical beam.

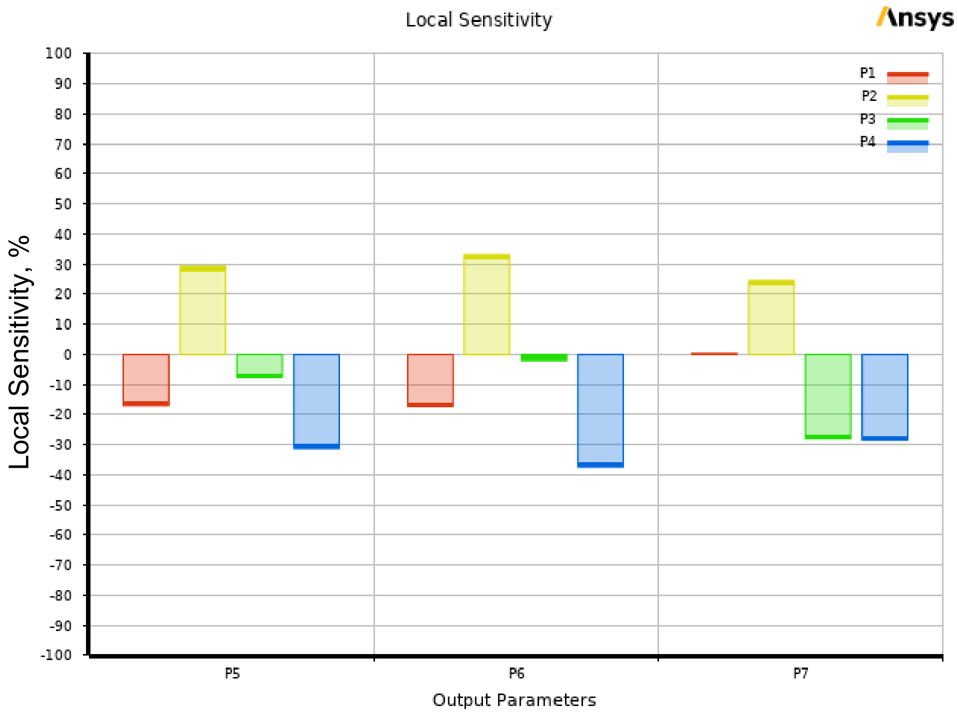

Fig. 5. Sensitivity diagram of optimized parameters:
*P*1 – *V*; *P*2 – *P*; *P*3 – *A*; *P*4 – *B*; *P*5 – *T*; *P*6 – σ_{yy}; *P*7 – σ_{zz}

Figure 6 illustrates the dependences of the maximum temperatures T and the maximum tensile stresses (σ_{yy} and σ_{zz}) on the input parameters within the treatment zone.

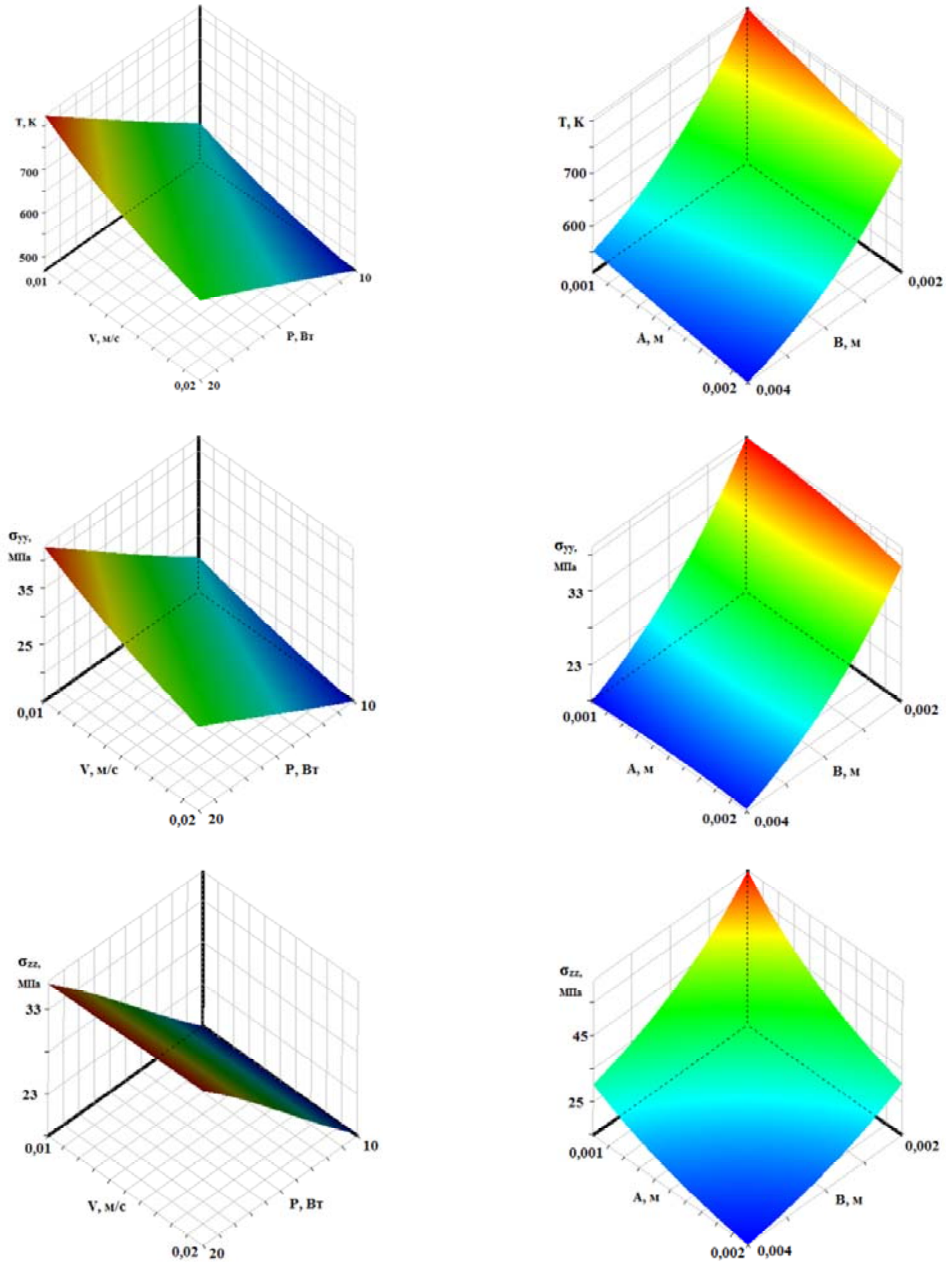

Fig. 6. Dependence of input parameters on output parameters

The study conducted a simulation of the laser cleaving process of silicate glasses through artificial neural networks, using the algorithm outlined in reference [17]. The results of finite element calculations performed in accordance with a numerical experiment design were used to prepare data for training and testing neural networks. In addition to the initial 25 combinations of the central compositional design, another 200 combinations were included.

The construction of neural networks containing two hidden layers (see Fig. 7) was performed using TensorFlow. The Adam optimizer, ReLU activation function, and MSE loss function were applied in the process of constructing the artificial neural network. The neural network underwent training for a total of 500 epochs. Consequently, 16 artificial neural networks were created with the number of neurons in two hidden layers ranging from 5 to 20, with an interval of 5.

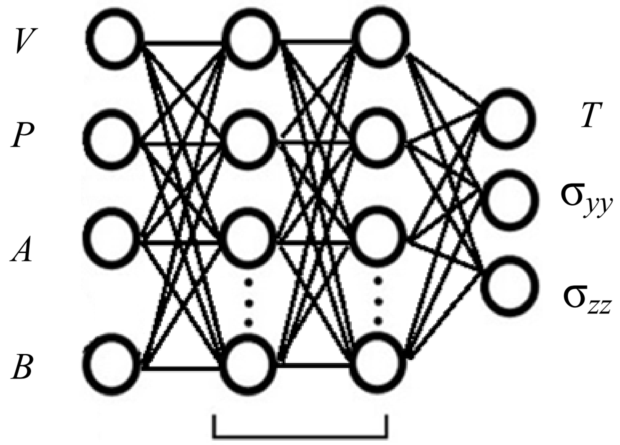

Fig. 7. Artificial neural network architecture

The dataset presented in Table 2 was used to perform tests on regression and neural network models.

Table 2

Test dataset

No.	*P*1 *V*, m/s	*P*2 *P*, W	*P*3 *A*, m	*P*4 *B*, m	*P*5 *T*, K	*P*6 σ_{yy}, MPa	*P*6 σ_{zz}, MPa
1	0.011	12	0.002	0.003	564	23.1	16.1
2	0.013	12	0.001	0.004	517	15.9	25.0
3	0.015	10	0.001	0.003	522	16.8	27.6
4	0.017	16	0.002	0.003	581	25.4	21.8
5	0.019	20	0.001	0.003	689	29.1	53.6
6	0.015	15	0.002	0.003	582	25.2	20.4
7	0.018	18	0.002	0.003	607	27.8	24.6
8	0.011	19	0.002	0.003	723	36.6	25.5
9	0.011	16	0.002	0.003	655	30.8	21.5
10	0.017	19	0.002	0.002	805	44.7	39.3

The resulting models were evaluated using mean absolute error (*MAE*), root mean square error (*RMSE*), mean absolute percentage error (*MAPE*), and determination coefficient R^2 [17].

Figure 8 shows heat maps illustrating the distribution of the mean absolute percentage error while estimating the maximum values of temperature and tensile stresses in the treatment zone of silicate glasses using elliptical beams. The number of neurons in the first and second hidden layers of the artificial neural network are shown by the vertical and horizontal axes, respectively. The intensity of color coding represents the extent of error: the error increases from light to dark. The artificial neural network with the architecture [5–15–15–15–2] demonstrated the most favourable results.

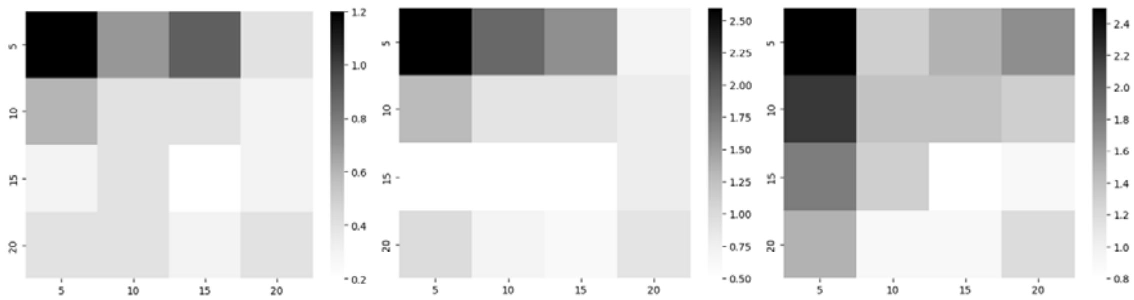

a) *b*) *c*)

Fig. 8. Heatmap of mean absolute percentage error distribution: when determining *T* (*a*); when determining σ_{yy} (*b*); when determining σ_{zz} (*c*)

Table 3 displays the estimation outcomes of both the regression and neural network models.

Table 3

Evaluation results of regression and neural network models

Criterion	Regression model			Neural network model		
	T	σ_{yy}	σ_{zz}	T	σ_{yy}	σ_{zz}
RMSE	1.7 K	0.29 MPa	0.29 MPa	1.5 K	0.12 MPa	0.28 MPa
MAE	2.3 K	0.41 MPa	0.41 MPa	0.9 K	0.14 MPa	0.21 MPa
MAPE	0.3 %	1.1 %	0.9 %	0.2 %	0.5 %	0.8 %
R^2	0.9993	0.9975	0.9984	0.9997	0.9996	0.9993

The evaluation findings of the generated models demonstrate a significant consistency with the outcomes obtained from finite element computations. The study revealed that the neural network model with the architecture [5–15–15–2] demonstrates superior efficacy in predicting the output parameters associated with the process of laser parallel splitting of silicate glasses.

The Ansys software module was used to optimize the parameters for parallel laser cleaving of silicate glass. The optimization procedures were conducted in accordance with the algorithm outlined in [20].

To optimize the parallel cleaving of silicate glass using the MOGA algorithm, the following criteria were chosen: $V \to \max$; $\sigma_{yy} \to \min$; $\sigma_{zz} \to \max$; $T \leq 789$ K.

The optimization results are provided in Table 4 (parameter values derived using the finite element method are presented in brackets).

Table 4

Optimization results

***P*1** *V*, m/s	***P*2** *P*, W	***P*3** *A*, m	***P*4** *B*, m	***P*5** *T*, K	***P*6** σ_{yy}, MPa	***P*6** σ_{zz}, MPa
0.02	19.7	0.001	0.0023	784 (786)	38.3 (38.4)	68.5 (68.4)

The application of the genetic algorithm provided a maximum relative error of less than 1 % when determining the maximum temperatures and maximum thermoelastic stresses generated in glass plates under the influence of elliptical laser beams on their surface.

Conclusion

This study presents the construction of regression models for parallel laser cleaving using the central composite design of numerical experimentation. An efficient artificial neural network architecture has been identified, which has superior prediction capabilities compared to regression models. The application of a genetic algorithm for optimization led to the determination of the laser cleaving modes of silicate glasses using elliptical beams in the plane parallel to the surface. These modes effectively facilitate the production of laser-induced cracks.

References

1. Nisar S. Laser glass cutting techniques – A review. *Journal of laser applications*, 2013, vol. 25, no. 4, pp. 042010-1–11.
2. Kondratenko V. S., Kudzh S. A. Precision Cutting of Glass and Other Brittle Materials by Laser-Controlled Thermo-Splitting (Review). *Glass and Ceramics*, 2017, no. 74, pp. 75–81. https://doi.org/10.1007/s10717-017-9932-1
3. Shalupaev S. V., Maksimenko A. V., Myshkovets V. N., Nikityuk Yu. V. Laser cutting of ceramic materials with a metallized surface. *Journal of Optical Technology*, 2001, vol. 68, no. 10, pp. 758–760. https://doi.org/10.1364/JOT.68000758
4. Shalupaev S. V., Shershnev E. B., Nikityuk Yu. V., Sereda A. A. Two-beam laser thermal cleavage of brittle nonmetallic materials. *Journal of Optical Technology*, 2006, vol. 73, no. 5, pp. 356–359. https://doi.org/10.1364/JOT.73.000356
5. Serdyukov A. N., Shalupaev S. V., Nikityuk Yu. V. Features of controlled laser thermal cleavage of crystalline silicon. *Crystallography Reports*, 2010, vol. 55, no. 6, pp. 933–937. https://doi.org/10.1134/S1063774510060064
6. Shalupaev S. V., Nikitjuk Yu. V., Sereda A. A., Aleksiejuk M. The analysis of laser thermosplitting of fragile materials by using of special geometry beams. *Archives of Metallurgy and Materials*, 2011, vol. 56, no. 4, pp. 1149–1155. https://doi.org/10.2478/v10172-011-0128-3
7. Serdyukov A. N., Shershnev E. B., Nikityuk Yu. V., Sholokh V. F., Sokolov S. I. Features of controlled laser thermal cleavage of crystal quartz. *Crystallography Reports*, 2012, vol. 57, no. 6, pp. 792–797. https://doi.org/10.1134/S1063774512060120
8. Shalupaev S. V., Serdyukov A. N., Mityurich G. S., Aleksiejuk M., Nikitjuk Yu. V., Sereda A. A. Modeling of mechanical influence of double-beam laser on single-crystalline silicon. *Archives of Metallurgy and Materials*, 2013, vol. 58, no. 4, pp. 1381–1385. https://doi.org/10.2478/amm-2013-0179
9. Zhao C., Zhang H., Yang L., Wang Y., Ding Y. Dual laser beam revising the separation path technology of laser induced thermal-crack propagation for asymmetric linear cutting glass. *International Journal of Machine Tools and Manufacture*, 2016, vol. 106, pp. 43–55. https://doi.org/10.1016/j.ijmachtools.2016.04.005
10. Wang H. L., Wang Y., Zhang H. Z., Wang X. W. Research Progress of Thermal Controlled Cracking of Hard-Brittle Plate. *Wuji Cailiao Xuebao,* 2018, vol. 33, no. 9, pp. 923–930. https://doi.org/10.15541/jim20170546
11. Shalupaev S. V., Shershnev E. B., Nikityuk Yu. V. Laser cleaving of glass in a plane parallel to the surface. *Proceedings of F. Skorina Gomel State University*, 2001, no. 6 (9), pp. 114–117.
12. Nikityuk Yu. V. Physical regularities of laser thermal cleaving of silicate glasses and alumina ceramics. Abstract of Ph. D. thesis. Minsk, 2009. 24 p.

13. Shalupaev S. V., Shershnev E. B., Nikityuk Yu. V. Laser thermal cleaving of dielectric materials. *Ceramics. Polish ceramic bulletin*, 2001, vol. 65, pp. 75–83.
14. Kondratenko V. S., Borisovsky V. Y., Naumov A. S., Sorokin A. V. New Technology of Laser Parallel Thermocracking of Brittle Materials. *Optics and Photonics Journal*, 2013, vol. 3, no. 2B, pp. 6–10. https://doi.org/10.4236/opj.2013.32B002
15. Parandoush P. A, Hossain A. A review of modeling and simulation of laser beam machining. *International Journal of Machine Tools and Manufacture*, 2014, no. 85, pp. 135–145.
16. Jiang P., Zhou Q., Shao X. *Surrogate model-based engineering design and optimization*. Singapore: Springer Publ., 2020. 240 p. https://doi.org/10.1007/978-981-15-0731-1
17. Bessmeltsev V. P., Bulushev E. D. Optimization of laser micro-processing modes, *Autometrics*, 2014, vol. 50, no. 6, pp. 3–21.
18. Nikitjuk Yu. V., Serdyukov A. N., Aushev I. Y. Determination of the parameters of two-beam laser splitting of silicate glasses using regression and neural network models. *Journal of the Belarusian State University*. Physics, 2022, no. 1, pp. 35–43. https://doi.org/10.33581/2520-2243-2022-1-35-43
19. Nikityuk Yu. V., Serdyukov A. N., Aushev I. Y. Optimization of laser cleaving parameters of quartz glass. *Problems of Physics, Mathematics and Technology*, 2021, no. 4 (49), pp. 21–28. https://doi.org/10.54341/20778708_2021_4_49_21
20. Nikityuk Yu. V., Baevich G. A., Myshkovets V. N., Maksimenko A. V., Aushev I. Y. Optimization of parameters of 12X18H9T steel processing using circular laser beams. *Vestnik of the Sukhoi State Technical University of Gomel*, 2022, no. 2, pp. 17–24.
21. Nikityuk Yu. V., Serdyukov A. N., Aushev I. Y. Optimization of two-beam laser cleavage of silicate glass. *Journal of Optical Technology*, 2022, vol. 89, no. 2, pp. 121–125. https://doi.org/10.1364/JOT.89.000121
22. Nikityuk Yu. V., Sereda A. A., Serdyukov A. N., Shalupaev S. V., Aushev I. Y. Parameters optimization of silicate glass two-beam asymmetric laser splitting. *Opticheskii Zhurnal*, 2023, vol. 90, no. 6, pp. 15–24. http://doi.org/10.17586/1023-5086-2023-90-06-15-24
23. Ansys.com – ANSYS official website (accessed 05.06.2023).
24. Kovalenko A. D. *Fundamentals of thermoelasticity*. Kiev, Naukova Dumka Publ., 1970. 308 p.
25. Machulka G. A. *Laser processing of glass*. Moscow, Sov. Radio Publ., 1979. 136 p.

Поступила 15.08.2023 г